JOURNAL OF SOLID STATE CHEMISTRY 51, 275–292 (1984)

Neutron Diffraction Structure Determination of the High-Temperature Form of Lithium Tritantalate, H-$LiTa_3O_8$

J. L. HODEAU AND M. MAREZIO

Laboratoire de Cristallographie, CNRS 166 X, 38042 Grenoble Cedex, France

AND A. SANTORO AND R. S. ROTH

National Measurement Laboratory, National Bureau of Standards, Washington, D.C. 20234, USA

Received December 9, 1982, and in revised form July 18, 1983

The crystal structure of H-$LiTa_3O_8$ has been reexamined by electron and neutron diffraction techniques. Neutron Weissenberg and electron diffraction photographs show that the space group of the compound is *Pmmn* and not *Pmma* as determined previously by X-ray diffraction techniques. There are eight molecules in the unit cell of lattice parameters a = 16.718(2) Å, b = 7.696(1) Å, c = 8.931(1) Å. These values show that the b axis of the new cell is doubled with respect to the parameter measured by X-rays. The structural refinement was based on 1074 independent reflections measured on a single crystal with a four-circle neutron diffractometer. The positions of all atoms, including the lithium atoms have been determined. The final R and wR factors were 0.036 and 0.035, respectively. The eight lithium cations occupy two sets of 4*f* positions (x, ¼, z) of the *Pmmn* space group. The ordering of four lithium ions over two sets of possible positions (4*j*) of space group *Pmma* is responsible for the doubling of the b axis. The other four Li^+ occupy two sets of positions (2*d*) of space group *Pmma*. All lithium ions are surrounded by 12 oxygen atoms arranged as cuboctahedra. The large thermal vibrations found for the lithium atoms and the ionic conductivity of H-$LiTa_3O_8$ at high temperatures are consistent with weak Li–O bonding.

Introduction

The synthesis of three crystallographic modifications of the compound $LiTa_3O_8$ was first reported by Roth *et al.* (*1*). The high-temperature form, designated as H-$LiTa_3O_8$, was found to be orthorhombic with a = 16.716 Å, b = 3.840 Å, and c = 8.941 Å. Since these cell dimensions are similar to those of $LiNb_6O_{15}F$, it was assumed that the two compounds were isostructural (*2*). $LiNb_6O_{15}F$ crystallizes in the *Pmma* space group with a = 16.635 Å, b = 3.964 Å, and c = 8.888 Å. Its structure was determined by single-crystal X-ray diffraction methods, but due to the small scattering factor of lithium, only the anion and the niobium positions were determined (*3*). The oxygen and fluorine ions form a framework built of octahedra and pentagonal bipyramids and the Nb^{5+} cations occupy the center of such polyhedra. The basic unit of this structure is a planar ring of five octahedra sharing corners. The space inside the ring is occupied by a pentagonal bipyramid. One such unit is shown as shaded in Fig. 1. It can be

0022-4596/84 $3.00

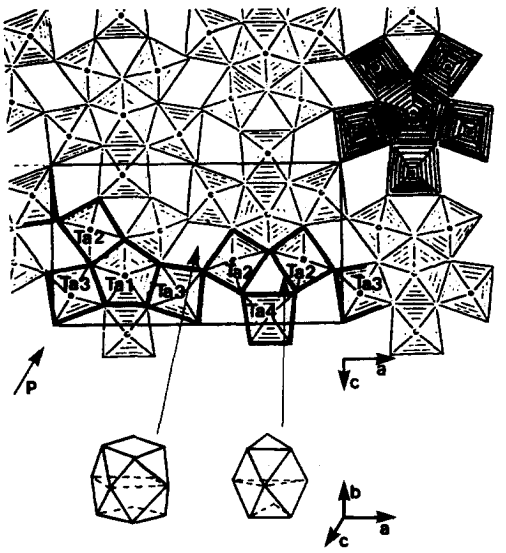

FIG. 1. Projection of the crystal structure of H-Li Ta_3O_8 along the *b* axis, showing the corner-sharing linkage of the units comprised of a pentagonal bipyramid surrounded by a five-octahedron ring. One of these units is shown as shaded. The unit-cell outline is marked. The numbering scheme for the tantalum cations is also given. Oxygen polyhedra enclosing the sites which could be occupied by the lithium cations are shown on the bottom.

seen that the octahedra share only corners among themselves, whereas each one of them shares an edge with the pentagonal bipyramid. The units are linked together by corner sharing to form layers. These layers are stacked along the third dimension by corner sharing, and each polyhedron shares a vertex with an equivalent one of the next layer (see Fig. 2). Thus the structure of $LiNb_6O_{15}F$ contains a three-dimensional array of corner-sharing octahedra, and therefore it is related to that of ReO_3. This relationship has been described by Hyde *et al.* (*4*). We would like to point out that in the ReO_3 structure the layers are formed by four-octahedron rings, whereas in $LiNb_6O_{15}F$, one-fifth, three-fifths, and one-fifth of the rings are five-octahedron, four-octahedron, and three-octahedron rings, respectively. The different stoichiometry of the $Nb_6O_{15}F^{1-}$ group with respect to ReO_3 is due to the filling of the pentagonal-ring centers with Nb^{5+} cations and to the extra oxygen atoms needed to form the pentagonal bipyramids. As stated above, the positions of the lithium atoms, which are needed to balance the electrostatic charge, were not determined. It was suggested that they probably occupy the large holes created by the corner-sharing octahedral array. Three-quarters of these holes are distorted cuboctahedra enclosed by 12 anions. The rest of the holes, which correspond to the three-octahedron rings, are enclosed by 9 anions forming three triangles: one above, one below, and one at the same level as the cation placed at the polyhedron center. The

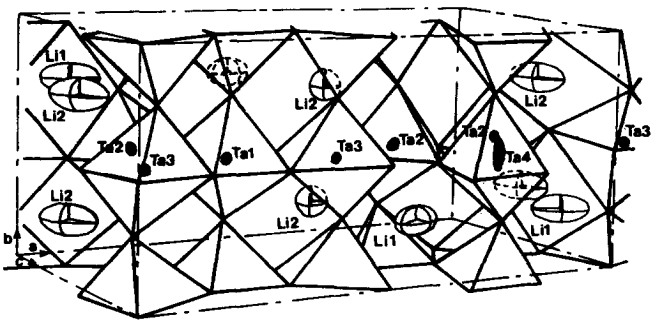

FIG. 2. Partial representation (only those polyhedra heavily outlined in Fig. 1 are shown) of a unit cell content for the H-$LiTa_3O_8$ structure, showing the corner-sharing linkage between layers. Cations are represented by the corresponding thermal ellipsoid.

difference between 12-coordinated and 9-coordinated sites is illustrated in Fig. 1.

The crystal structure of H-$LiTa_3O_8$ has been refined independently by two groups. Nord and Thomas (*5*) used X-ray single-crystal and neutron powder diffraction data, whereas Fallon *et al.* (*6*) used only X-ray single-crystal data. Both groups refined the structural parameters of the $[Ta_3O_8]^{1-}$ anion in the *Pmma* space group and confirmed its similarity to the $[Nb_6O_{15}F]^{1-}$ anion. However, they failed to locate unequivocally the lithium ions. Nord and Thomas noticed, during the refinement based on X-ray single-crystal data, that one of the tantalum atoms, namely Ta(4), acquired an anomalously large thermal vibrational along the *b* axis. This was interpreted as an indication that the structure did not contain the center of symmetry. Since statistical and piezoelectric tests failed to produce any definite conclusion, the subsequent refinements were still carried out in the *Pmma* space group; however, the Ta(4) atoms were split to lie disordered on either side of the mirror plane at $y = 0$. Although the difference in scattering power for tantalum, oxygen, and lithium is much more favorable for neutron than for X-ray diffraction, total-profile analysis based on neutron powder data gave somewhat unreasonable positions for the lithium atoms. Fallon *et al.* (*6*) suggested that the four lithium atoms per unit cell occupied the 12-coordinated sites corresponding to (4*j*) positions of space group *Pmma*. Their suggestion was based on an analysis of the O–O distances of the anion framework. Another attempt to position the lithium atoms in the structure of H-$LiTa_3O_8$ was made by Werner *et al.* (*7*), who refined the structures of $Li_{1-x}Ta_3O_{8-x}F_x$ (with $x = 0$, 0.25, and 0.50) by total-profile analysis of Guinier–Hägg X-ray powder-film data. From sequential changes in interatomic distances and disorder within the series, these authors proposed that the four lithium atoms occupy the (4*j*) $(x, \frac{1}{2}, z)$ positions with $x = 0.11$, $y = \frac{1}{2}$, and $z = 0.03$. These positions, which correspond to one type proposed by Nord and Thomas (*5*), are inside the 12-coordinated polyhedra whose center had been suggested by Fallon *et al.* (*6*).

The conduction properties of H-$LiTa_3O_8$ have been studied by Réau *et al.* (*8*) by the complex-impedance method, which revealed the ionic character of the conductivity. The values of $6 \times 10^{-4}\ \Omega^{-1}\ cm^{-1}$ and 0.78 eV are given for the conductivity at 300°C and the activation energy, respectively. These authors attributed this conductivity to the movement of the lithium ions. Subsequently, Magniez (*9*) showed that the conductivity is isotropic. Réau *et al.* (*10*) investigated the variation of the ionic conductivity for the solid solutions $Li_{1-x}Ta_3O_{8-x}F_x$ and $Li_{1-x}Ta_{3-x}W_xO_8$ as a function of x. The ionic conductivity of the F-substituted $LiTa_3O_8$ compounds has a maximum for $x = 0.75$, while for both compounds the curve of the activation energy has a minimum for the same value of x.

To solve the problem of the lithium arrangement in the structure of H-$LiTa_3O_8$, necessary to propose a model for the ionic-conduction mechanism, large single crystals suitable for neutron diffraction have been synthesized. Since the previous refinements of H-$LiTa_3O_8$ and of isostructural compounds carried out in the *Pmma* space group had indicated the existence of disorder, electron diffraction photographs were taken. They revealed that, in order to index all the spots, a doubling of the *b* parameter was necessary. This superstructure was confirmed by single-crystal film neutron data taken with a Weissenberg camera (*11*). The present article reports the electron diffraction and neutron Weissenberg data together with the results of two structural refinements with the new unit cell, the first based on neutron single-crystal diffraction data, and the second based on the profile analysis of neutron powder diffraction data.

Powder Sample and Single-Crystal Preparations

Powder samples of H-$LiTa_3O_8$ were prepared by grinding together 1 : 1 mole-ratio mixtures of $LiTaO_3$ and Ta_2O_5. These batches were fired in Pt crucibles at 1000°C for several days, reground and refired several times at temperatures varying from 1250°C to about 1500°C, and then quenched in air or in vacuum. The degree of combination and crystallinity of the samples was checked by the use of a X-ray powder diffractometer using Cu$K\alpha$ radiation and a graphite monochromator.

Single crystals of H-$LiTa_3O_8$ were obtained by the Czochralski technique by pulling from a melt, kept above 1650°C, of the same composition as the powder samples. Each boule was pulled from a seed obtained from an earlier pull. The seed was tied to an iridium rod, and the melt was contained in an iridium crucible in an air atmosphere with the O_2 content depleted by flowing argon around the insulators surrounding the crucible. To investigate the effect of the cooling rate upon the ordering of the lithium atoms, four types of single crystals were prepared. For the first and second types, a boule was annealed at 1200°C for 3 hr in an unsealed and a sealed Pt tube, respectively. The tubes were then cooled in air at the rate of 2°C/min. For the third and fourth samples, a boule was heated at 1450°C for 6 hr in an unsealed and a sealed Pt tube, respectively. The tubes were then quenched in H_2O. As the fourth sample was sealed in a Pt tube, the water did not touch the crystal. The quality of the crystals was checked by taking X-ray precession photographs with Mo$K\alpha$ radiation.

The lattice parameters for each batch were determined from powder data taken with a Guinier camera and Fe$K\alpha$ radiation. A silicon standard was used. The values obtained were all the same and in good agreement with those quoted by Werner *et al.* (*7*) (a = 16.702 Å, $2b$ = 7.697 Å, c = 8.934 Å). The values obtained for the second batch, from which the crystal used in the intensity data collection was taken, were a = 16.718(2) Å, b = 7.696(1) Å, c = 8.931(1) Å.

Electron Diffraction Studies

The electron diffraction studies were carried out at CSIC in Madrid on a Siemen's Elmiskop-102 microscope. The microscope was operated at 100 kV and equipped with a double tilting goniometer stage in order to reach different planes in reciprocal space with the same sample. Samples for study were crushed in an agate mortar and suspended in *n*-butanol, then transferred to holey carbon-coated copper grids.

Several planes of the reciprocal lattice were explored and photographed for each sample. An example is given in Fig. 3 which shows the reciprocal net perpendicular to the $[02\bar{1}]$ zone axis. The two perpendicular rows in the plane of the photograph are [100]* and [012]*, respectively. Rows of extra spots parallel to the [100]* row are readily visible and indicate a superstructure. All spots can be indexed if one doubles the b axis of the orthorhombic unit cell determined by X-ray diffraction. All photographs corresponding to different planes of the reciprocal lattice showed that the doubling of the b axis was necessary in order to index all the spots appearing on the films.

X-Ray Diffraction Precession Studies

Precession photographs were obtained using Mo$K\alpha$ radiation. Exposures longer than 4 days failed to reveal the superstructure reflections. This strongly indicated that the superstructure was due to the positions of the lithium atoms and that the contribution from the $Ta_3O_8^{1-}$ framework was negligible. In fact, for X-ray diffraction the ratio of the atomic scattering factors of lithium with respect to that of tantalum is 0.04 at

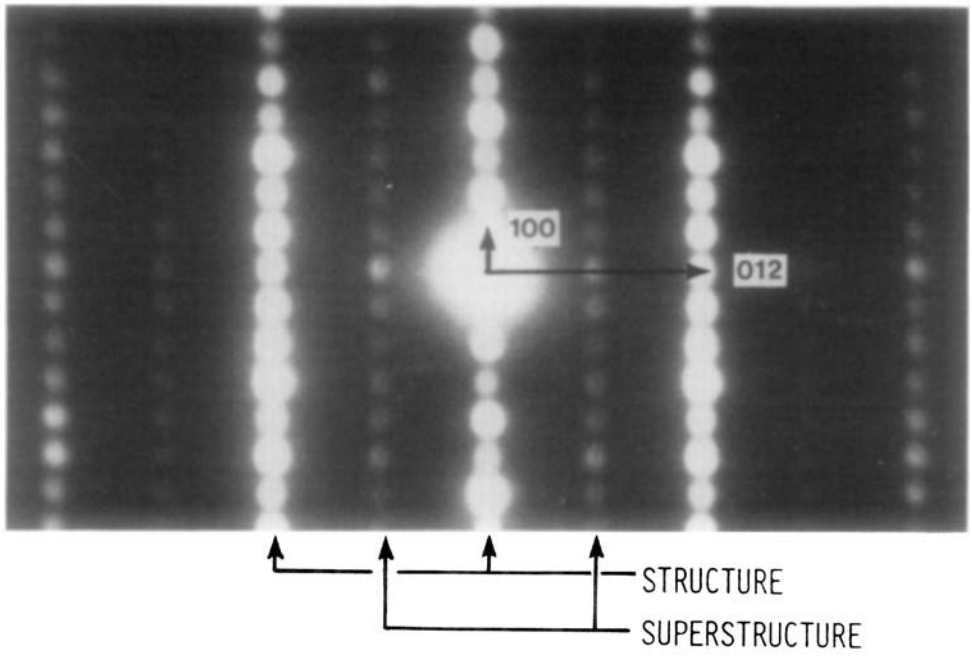

FIG. 3. Electron diffraction photograph showing the reciprocal plane perpendicular to the $[02\bar{1}]$ zone axis. The Miller indices correspond to the unit cell determined by X-ray diffraction. The superstructure rows are indicated.

sin $\theta/\lambda = 0$ and decreases for increasing sin θ/λ. Since the corresponding ratio for neutron diffraction is 0.31 and does not vary with sin θ/λ, the space symmetry of the supercell was determined from the single-crystal neutron diffraction data.

Neutron Diffraction Weissenberg Data

The neutron diffraction Weissenberg photographs were obtained with the Weissenberg camera at the Laue-Langevin Institute in Grenoble. The samples were single crystals whose volume varied between 1 and 4 mm^3. A 1.71-Å wavelength was used. The crystals were oriented with the *b* or *c* axis along the rotation axis, and the equi-inclination geometry was used in all cases. Figure 4 shows the photograph of the *hk*0 layer. The continuous lines represent the reciprocal lattice corresponding to the unit cell determined by X-ray diffraction. Strong spots are visible between the $[hk0]^*$ and $[h, k + 1, 0]^*$ rows, whose indices are $[h, (2k + 1)/2, 0]^*$. This photograph, as well as those of the upper levels, demonstrates that the *b* axis determined by X-ray diffraction must be doubled. The new systematic absences occurred for the *hk*0 reflections with $h + k = 2n + 1$, and therefore, the possible space groups are *Pmmn* and $Pm2_1n$. Table I shows the new positions of the atoms in the asymmetric unit for space group *Pmmn*. All possible sites for the lithium atoms are included. The positions corresponding to space group *Pmma* are given for comparison.

At least one crystal from each of the four different preparations was investigated. The intensity ratios between the reflections of the superstructure and those of the basic structure were determined visually and did not vary from sample to sample. It was therefore assumed that the cooling history

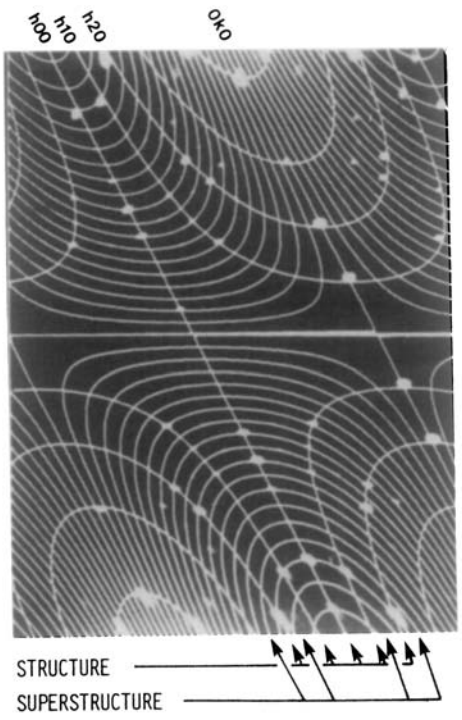

FIG. 4. Neutron diffraction Weissenberg photograph corresponding to the [001] zone. The reciprocal lattice lines of the X-ray unit cell are outlined. The superstructure rows are indicated. The pull symmetry of the pattern is not apparent in the figure because some of the spots were intercepted by the beam stop. The $\bar{2}00$ reflection, for example, is not visible for this reason.

does not have any significant effect upon the ordering of the lithium atoms.

Neutron Diffraction Powder Data

Neutron diffraction powder data were collected with a five-detector diffractometer at the National Bureau of Standards reactor. The conditions used in the experiment are summarized in Table II. The neutron intensities were analyzed with the Rietveld method, modified by Prince (*12*), in order to simultaneously process the data from the five counters of the diffractometer. The background was assumed to be a straight line of finite slope and was refined for each of the five channels of the diffractometer together with the profile and structural parameters. The initial values of the lattice parameters were those determined by X-ray powder diffraction (*7*), with the b axis doubled. The profile parameters U, V, and W, which define the full width a half maximum of the Bragg reflections, were calculated with the formulae derived by Caglioti *et al.* (*13*). The neutron scattering amplitudes used in the refinements were $b(\mathrm{Ta}) = 0.70$, $b(0) = 0.58$, and $b(\mathrm{Li}) = -0.214 \times 10^{-12}$ cm (*14*). In all cases a refinement was considered complete when the factor R_W did not change by more than one part in a thousand in two successive cycles. The centrosymmetric space group *Pmmn* was used. The initial positions of the oxygen and tantalum atoms were those given by Nord and Thomas (*5*). They were transformed to take into account the doubling of the b axis. The lithium atoms were not included. Values of 0.3 and 0.5 Å^2 were assigned to the temperature factors of the tantalum and oxygen atoms, respectively. Initially only the scale factor and the lattice and profile parameters were refined, while all positional and thermal parameters were kept fixed. Subsequently, with the Ta(4) placed in the position (0.25, 0.05, 0.05), the positional parameters of the 0(10) and 0(101) atoms, which correspond to the apices of the octahedron around Ta(4), were refined. The Ta(4) atom lies on the mirror plane at $y = 0$ of the old unit cell; however, as mentioned above, Nord and Thomas (*5*) had found a large improvement in the R factor by moving Ta(4) out of the mirror plane. This shift of about 0.4 Å along the b axis represents the only a priori distortion imposed on the present refinement. The subsequent stages of refinement consisted in varying, sequentially, all positional parameters of the atoms lying on the plane at about $y = 0$ and all positional parameters of the atoms lying on the plane at $y = \frac{1}{4}$. There are eight lithium atoms per unit cell which

TABLE I

ATOMIC POSITIONS IN SPACE GROUPS *Pmma* AND *Pmmn*

Pmma a = 16.702 Å, b = 3.8485 Å, c = 8.9340 Å; 4 molecules per unit cell						*Pmmn* a = 16.702 Å, b = 7.6970 Å, c = 8.9340 Å; 8 molecules per unit cell					
Ta(1)	2*e*	*mm*	¼	0	*z*	Ta(1)	4*e*	*m*	¼	*y*	*z*
Ta(2)	4*i*	*m*	*x*	0	*z*	Ta(2)	8*g*	1	*x*	*y*	*z*
Ta(3)	4*i*	*m*	*x*	0	*z*	Ta(3)	8*g*	1	*x*	*y*	*z*
Ta(4)	2*e*	*mm*	¼	0	*z*	Ta(4)	4*e*	*m*	¼	*y*	*z*
O(1)	2*e*	*mm*	¼	0	*z*	O(1)	4*e*	*m*	¼	*y*	*z*
O(2)	4*i*	*m*	*x*	0	*z*	O(2)	8*g*	1	*x*	*y*	*z*
O(3)	4*i*	*m*	*x*	0	*z*	O(3)	8*g*	1	*x*	*y*	*z*
O(4)	2*f*	*mm*	¼	½	*z*	O(4)	2*a*	*mm*	¼	¼	*z*
						O(41)	2*b*	*mm*	¼	¾	*z*
O(5)	4*i*	*m*	*x*	0	*z*	O(5)	8*g*	1	*x*	*y*	*z*
O(6)	4*i*	*m*	*x*	0	*z*	O(6)	8*g*	1	*x*	*y*	*z*
O(7)	4*j*	*m*	*x*	½	*z*	O(7)	4*f*	*m*	*x*	¼	*z*
						O(71)	4*f*	*m*	*x*	¾	*z*
O(8)	2*a*	2/*m*	0	0	0	O(8)	4*c*	$\bar{1}$	0	0	0
O(9)	4*j*	*m*	*x*	½	*z*	O(9)	4*f*	*m*	*x*	¼	*z*
						O(91)	4*f*	*m*	*x*	¾	*z*
O(10)	2*f*	*mm*	¼	½	*z*	O(10)	2*a*	*mm*	¼	¼	*z*
						O(101)	2*b*	*mm*	¼	¾	*z*
Li(1)	4*j*	*m*	*x*	½	*z*	Li(1)	4*f*	*m*	*x*	¼	*z*[a]
						Li(11)	4*f*	*m*	*x*	¾	*z*
Li(2)	2*d*	2/*m*	0	½	½	Li(2)	4*f*	*m*	*x*	¼	*z*
Li(3)	2*f*	*mm*	¼	½	*z*	Li(3)	2*a*	*mm*	¼	¼	*z*
						Li(31)	2*b*	*mm*	¼	¾	*z*

[a] For simplicity, the sites of Li(1), Li(11), Li(2), Li(3), and Li(31) are sometimes called, in the text, sites 1, 11, 2, 3, and 31, respectively.

TABLE II

EXPERIMENTAL CONDITIONS USED TO COLLECT THE NEUTRON POWDER INTENSITY DATA FOR H-$LiTa_3O_8$

Monochromatic beam:	reflection 220 of a Cu monochromator	
Wavelength:	1.5416(3) Å	
Horizontal divergences:	(a) in-pile collimator:	10′ arc
	(b) monochromatic beam collimator:	20′ arc
	(c) diffracted beam collimator:	10′ arc
Monochromator mosaic spread:	~15′ arc	
Sample container:	vanadium can ~10 mm in diameter	
Angular ranges scanned by each detector:	10–40, 30–60, 50–80, 70–100, 90–120	
Angular step:	0.05°	

may occupy twice as many possible sites. These atoms were introduced in the refinement with starting positional parameters corresponding to the centers of the respective polyhedra, with a fixed temperature factor of 1 $Å^2$ and with an initial zero value for the occupancy factors, which were allowed to vary. During the last stage of refinement, the scale factor and the lattice and profile parameters were varied together with the positional parameters of all atoms, with the occupancy factor of the lithium atoms, and with the overall temperature factor, while the individual temperature factors for the tantalum, oxygen, and lithium atoms were kept fixed at 0.3, 0.5, and 1.0 $Å^2$, respectively. The final R factors[1] were $R_N = 7.17$, $R_P = 6.17$, $R_W = 8.36$, and $R_E = 4.06$. The final parameters are given in Table III. The occupancy factors of the lithium atoms did not correspond exactly to the stoichiometric formula $LiTa_3O_8$ with eight lithium atoms per unit cell. A few cycles of refinement were then tried in which the occupancy factors of the lithium atoms were kept fixed at the nearest values corresponding to the stoichiometric formula, namely, 1.0, 0.0, 0.5, 0.0, and 1.00 for Li(1), Li(11), Li(2), Li(3), and Li(31), respectively. No noticeable change in the structural parameters and in the R factors was obtained. We assumed, therefore, that the sites of Li(1) and Li(31) were fully occupied, the site of Li(2) was half occupied, and the other two sites were empty.

It should be pointed out that in the neutron powder pattern there exist three reflections with measurable intensity at about 21.4, 31.8, and 34.2° 2θ. These reflections have either zero or almost zero calculated intensity. Refinements carried out by excluding the regions around these reflections ($20.8 \leq 2\theta \leq 22.0$ and $31.2 \leq 2\theta \leq 35.0$) decreased the R_N, R_P, R_W, and R_E factors from 7.17, 6.17, 8.36, and 4.06 to 5.59, 5.76, 7.35, and 4.01, respectively, and the differences in the structural parameters were always less than one standard deviation. Furthermore, the extra reflections do not exist in the powder pattern of another sample. These results indicate that the extra reflections may be due to impurities or to inhomogeneities in the samples. Possible impurities would be L-$LiTa_3O_8$, M-$LiTa_3O_8$, $LiTaO_3$, and Ta_2O_5. However, the extra lines do not belong to any of these compounds.

[1] The R factors used in profile analysis are defined in a number of publications; see, for example, Ref. (*15*).

Single-Crystal Neutron-Diffraction Data

Single-crystal intensity data were collected on a spherical sample of 0.25 cm in diameter mounted on a four-circle neutron diffractometer at the National Bureau of Standards reactor. The crystal from which the sphere was ground came from the second preparation batch. A 1.273-Å wavelength was used. All reachable reflections in the θ interval of 7–60° were measured by the $\theta/2\theta$ scan technique in the interval $\Delta 2\theta = (3.5 + 3.5 \tan \theta)$ and in steps of 0.1°. The background was measured at each end of the scan interval by averaging over 10 points on each side. A total of 4865 reflections were measured. Reflections with $F < 6\sigma(F)$ were considered unobserved. This criterion reduced the number of measured reflections to 2714, and a total of 1074 and 1746 independent reflections in the *mmm* and *m2m* point groups, respectively. The average standard deviations calculated for the equivalent reflections were 2.8% for *mmm* and 2.6% for *m2m*, which indicates that the difference in intensity between Friedel pairs was of the same order of magnitude in the two point groups. Therefore, the structure was first refined in the centric space group. Since for the sphere used $\mu R = 0.08$, no absorption correction was applied.

TABLE III

FINAL POSITIONAL AND THERMAL PARAMETERS FOR THE STRUCTURE OF H-$LiTa_3O_8$[a]

	x	y	z	U_{11}	U_{22}	U_{33}	U_{12}	U_{13}	U_{23}
Ta(1)	0.25	0.0012(3)	0.6878(2)	0.0054(8)	0.0061(9)	−0.0003(10)	0.00	0.00	−0.0005(9)
	0.25	−0.003(2)	0.690(1)	0.0038					
Ta(2)	0.13256(7)	−0.0011(2)	0.3930(2)	0.0057(5)	0.0071(6)	0.0010(7)	0.0015(5)	−0.0002(5)	−0.0001(6)
	0.1312(5)	0.010(2)	0.3944(7)	0.0038					
Ta(3)	0.06024(7)	−0.0004(2)	0.8114(2)	0.0041(5)	0.0038(6)	0.0028(7)	0.0005(5)	0.0004(5)	0.0003(8)
	0.0609(5)	−0.001(1)	0.8076(9)	0.0038					
Ta(4)	0.25	0.0025(4)	0.0539(2)	0.0055(8)	0.0451(14)	0.0004(10)	0.00	0.00	0.0048(14)
	0.25	0.018(2)	0.056(1)	0.0038					
O(1)	0.25	−0.0249(3)	0.4530(3)	0.0039(9)	0.0079(11)	0.0007(12)	0.00	0.00	0.0008(10)
	0.25	−0.023(2)	0.453(1)	0.0063					
O(2)	0.13163(8)	0.0013(2)	0.6202(2)	0.0052(6)	0.0098(7)	0.0003(8)	−0.0007(6)	0.0011(7)	−0.0005(8)
	0.1315(6)	0.008(2)	0.6203(9)	0.0063					
O(3)	0.17483(9)	0.0259(2)	0.8779(2)	0.0046(6)	0.0077(8)	0.0025(9)	0.0001(5)	0.0002(7)	−0.0007(8)
	0.1743(5)	0.029(2)	0.8791(8)	0.0063					
O(4)	0.25	0.25	0.6716(6)	0.0104(16)	0.0018(14)	0.0071(24)	0.00	0.00	0.00
	0.25	0.25	0.668(2)	0.0063					
O(41)	0.25	0.75	0.7041(6)	0.0101(16)	0.0011(14)	0.0080(25)	0.00	0.00	0.00
	0.25	0.75	0.710(2)	0.0063					
O(5)	0.16236(10)	−0.0404(2)	0.1883(2)	0.0091(8)	0.0156(9)	0.0051(10)	−0.0004(6)	0.0036(7)	0.0018(8)
	0.1639(6)	−0.044(1)	0.191(1)	0.0063					
O(6)	0.02035(9)	0.0393(2)	0.3404(2)	0.0043(7)	0.0087(7)	0.0076(10)	0.0007(6)	−0.0035(7)	−0.0012(7)
	0.0200(5)	0.041(1)	0.332(1)	0.0063					
O(7)	0.1416(2)	0.25	0.3959(4)	0.0170(12)	0.0031(10)	0.0157(18)	0.00	−0.0083(14)	0.00
	0.1524(8)	0.25	0.387(2)	0.0063					
O(71)	0.1048(2)	0.75	0.4151(4)	0.0109(11)	0.0014(10)	0.0092(18)	0.00	−0.0029(12)	0.00
	0.111(1)	0.75	0.413(1)	0.0063					
O(8)	0.00	0.00	0.00	0.0169(11)	0.0106(10)	0.0039(13)	−0.0021(10)	0.0087(10)	−0.0031(13)
	0.00	0.00	0.00	0.0063					
O(9)	0.0417(2)	0.25	0.8038(4)	0.0153(13)	0.0015(10)	0.0109(17)	0.00	0.0002(12)	0.00
	0.047(1)	0.25	0.817(2)	0.0063					
O(91)	0.0731(1)	0.75	0.8425(4)	0.0093(11)	0.0010(9)	0.0264(22)	0.00	0.0026(12)	0.00
	0.0792(9)	0.75	0.852(2)	0.0063					
O(10)	0.25	0.25	0.0932(6)	0.0167(18)	0.0098(16)	0.0123(27)	0.00	0.00	0.00
	0.25	0.25	0.082(2)	0.0063					
O(101)	0.25	0.75	0.0161(7)	0.0266(21)	0.0132(19)	0.0159(30)	0.00	0.00	0.00
	0.25	0.75	0.024(2)	0.0063					
Li(1) (f.o.)	0.9163(12)	0.25	0.9083(21)	0.117(12)	0.032(6)	0.065(13)	0.00	0.040(11)	0.00
(f.o.)	0.910(2)	0.25	0.952(4)	0.0127					
Li(2) (f.o.)	−0.0063(10)	0.25	0.462(3)	0.076(9)	0.038(6)	0.114(20)	0.00	0.052(11)	0.00
(h.o.)	0.000(6)	0.25	0.539(7)	0.0127					
Li(31)	—	—	—	—	—	—	—	—	—
(h.o.)	0.25	0.25	0.304(6)	0.0127					

[a] For each atom the first line gives the parameters of the single crystal refinement and the second one gives those of the powder refinement. In the powder experiment only isotropic thermal parameters were considered.

Note. f.o.—full occupied; h.o.—half occupied.

The starting values for the positional, thermal, and occupancy parameters for the first stage of refinement were those determined by the powder neutron diffraction data. After a few cycles it was noticed that the occupancy parameters of Li(2) and Li(31) had changed drastically. The former had increased from ~0.5 to ~1.0, while the latter had decreased from ~1.0 to ~0.0. The R and wR factors were 0.13 and 0.16, respectively. A comparison of F_{obs} and F_{calc} values showed that the extinction effects were appreciable. A refinement in space group $Pm2_1n$ gave positional parameters not significantly different from the centrosymmetrical positions, and several thermal parameters became negative. These results indicate that the structure of H-$LiTa_3O_8$ is

TABLE IV

E VALUES FOR THE POWDER AND SINGLE-CRYSTAL REFINEMENTS

	E_x	E_y	E_z
Ta(1)	—	−1.6	2.2
Ta(2)	2.7	2.5	2.0
Ta(3)	1.3	0.6	−4.1
Ta(4)	—	7.6	2.1
O(1)	—	−0.9	0.0
O(2)	−0.2	3.3	0.1
O(3)	−1.0	1.5	1.5
O(4)	—	—	−1.7
O(41)	—	—	2.8
O(5)	2.4	−3.5	2.7
O(6)	−0.5	1.7	−8.2
O(7)	13.1	—	−4.4
O(71)	6.1	—	−2.0
O(8)	—	—	—
O(9)	5.2	—	6.5
O(91)	6.7	—	4.7
O(10)	—	—	−5.4
O(101)	—	—	3.7
Li(1)	−2.7	—	9.7
Li(2)	−1.0	—	10.1

centrosymmetric and are consistent with the good agreement obtained between intensities of Friedel pairs.

The final refinements were carried out by using the LINEX program, which includes the extinction correction derived by Becker and Coppens (*16*). These refinements were based on all 1074 reflections, each weighted by $1/\sigma^2(F)$. The scale and extinction factors, the positional and anisotropic thermal parameters of all atoms, and the occupancy factors of the Li sites were varied. After convergence was attained, the occupancy factors were less than 3% for Li(11), Li(3), and Li(31) and ~85% for Li(1) and Li(2). The values of the extinction coefficients indicated that the extinction effects were due to the mosaic spread rather than to the dimensions of the mosaic domains. Both Gaussian and Lorentzian mosaic distributions were tried, and the g values in the two cases were 5.6×10^{-5} and 8.5×10^{-5}, respectively. The former corresponds to a spread of 10″, while the latter to one of 4″. During the last cycles of refinement, the occupancy factors of those oxygen atoms which had anomalously larger temperature factors were allowed to vary, while the Ta(4) atom was allowed to move out of its centrosymmetrical position. However, the occupancy factor of the oxygen atoms remained close to unity, and the positional parameters of Ta(4) did not shift appreciably. The best refinement was obtained with full occupany for all oxygen atoms and for Li(1) and Li(2), and with a Lorentzian mosaic spread. The R and wR factors were 0.036 and 0.035, respectively. The final positional and thermal parameters are given in Table III where they are compared with the results of the powder refinement.

Comparison between the Powder and Single-Crystal Refinements

The powder and single-crystal refinements yield different ordering for the lithium atoms. Since the neutron diffraction Weissenberg data indicated that this ordering does not depend upon the sample preparation, one of the two results should be incorrect. The powder and single-crystal refinements give different positions for one-fourth of the lithium atoms and, in addition, are not in satisfactory agreement for the other positional parameters. A comparison can be done by calculating for each parameter the value $E = \Delta/\sqrt{\sigma_1^2 + \sigma_2^2}$, where Δ is the difference between two corresponding parameters and σ_1 and σ_2 are the standard deviations. A good agreement corresponds to $|E| \leq 1$. As can be seen from Table IV, the E values vary between 7.6 and 0.6 for the tantalum atoms, between 13.1 and 0.0 for the oxygen atoms, and between 10.1 and 1.0 for the lithium atoms. To see whether the powder refinement had reached a false minimum, which would explain the large E values, an additional refinement based on powder data was carried

out using as initial values of the structural parameters those obtained in the single-crystal refinement. The eight lithium atoms were placed in sites 1 and 2, while their occupancy factors were fixed at 1.0 and were not varied. After convergence was attained, the R factors were 7.67, 6.42, 8.60, and 4.09 for R_N, R_P, R_W, and R_E, respectively. These values are slightly higher than those obtained in the previous powder refinement (7.17, 6.17, 8.36, 4.06). The E values calculated for the two powder refinements are all ~1, except the one corresponding to the z parameter of O(91), which is 4.3 and, as expected, those corresponding to the x and z parameters of Li(2), which are 3.3 and 10.9, respectively. The large E value for O(91) is probably a consequence of the full occupancy of the Li(2) sites. In fact, O(91) belongs to the coordination polyhedron around Li(2), and therefore a large correlation between the occupancy factor of Li(2) and the positional parameters of O(91) should be expected. The small difference between the two sets of R factors and the small E values indicate that the powder data are not very sensitive to the lithium contribution.

Because of their different definition, the R factors of the powder and single-crystal refinements cannot be compared. Thus the criterion that one can use to determine which of the two refinements is the correct one must be based on the standard deviations. As can be seen from Table III, the standard deviations of the positional parameters yielded by the single-crystal refinement are usually smaller, by a factor ranging between 3 and 10, than those obtained by the powder refinement. This indicates that the refinement based on single-crystal data yields more precise results than those based on powder data, and therefore the lithium ordering obtained by the former refinement should be considered as the correct one. The reason why the powder refinement yielded wrong positions for one-fourth of the lithium atoms may be due to the presence of impurities and/or inhomogeneities in the sample and also to the fact that the large and very anisotropic temperature factors of the lithium atoms were not refined because of the limited number of intensity data.

Discussion

The departure from the *Pmma* space symmetry and the doubling of the b axis are due to the ordering of half the lithium cations. In the supercell the eight positions 2(4*j*) of *Pmma* are split into two sets of four positions and only one of these two sets is fully occupied by the lithium cations. As can be seen from Table III, the lowering of the crystal symmetry does not have any appreciable effect on the distribution of the tantalum ions. All displacements of the tantalum cations from the mirror plane at $y = 0$ are less than 0.02 Å. However, the displacements of the oxygen ions can be as much as 0.34 Å.

As has been stated above, there exists a relationship between H-$LiTa_3O_8$ and $LiNb_6O_{15}F$. For instance, the frameworks, of $Ta_3O_8^{1-}$ and of $Nb_6O_{15}F^{1-}$, have almost identical arrangements. However, without knowing the lithium positions in the latter compound, one cannot determine whether or not the two compounds belong to the same space group. If in the structure of $LiNb_6O_{15}F$ the sites 2*d* or 2*f* are occupied by Li(2) or Li(3), then the doubling of the b axis is not needed and the structure would have the *Pmma* space symmetry. On the contrary, if the Li(1) occupy the sites 4*j*, then the ordering might take place either with Li(1) or with Li(11) in sites 4*f* and both structures would have the same space symmetry, namely *Pmmn*.

Figures 5 and 6 represent two projections of the H-$LiTa_3O_8$ structure on the (010) and (001) planes, respectively. The oxygen polyhedra around the tantalum cations are

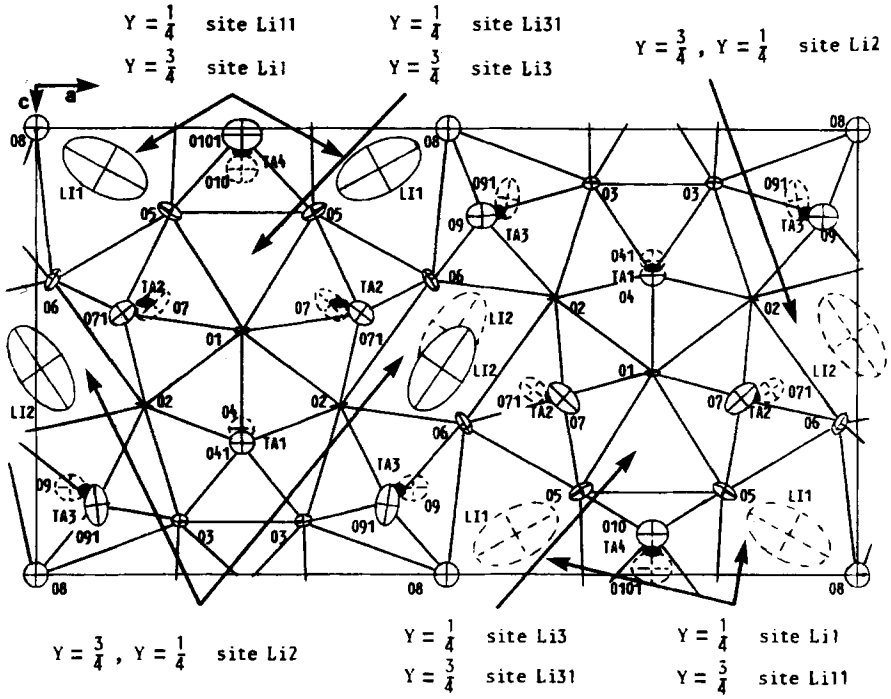

FIG. 5. Projection of the crystal structure of H-$LiTa_3O_8$ along the *b* axis. Each atom is represented by the section of the thermal ellipsoid perpendicular to the *b* axis. Oxygen polyhedra around the tantalum cations are outlined. All possible lithium sites with the heights along the *b* axis are given.

outlined. The corresponding interatomic distances are given in Table V. They were calculated by the use of the X-ray powder lattice constants (*7*) and the positional parameters of the LINEX refinement. The average Ta–O distance of the pentagonal-bipyramidal site is 2.049 Å (coordination number 7), while the overall average of the Ta–O distance for the octahedral sites (coordination number 6) is 1.978 Å. The Li(1) and Li(2) cations are surrounded by 12 oxygen anions arranged as cuboctahedra. The individual Li–O distances vary over such a large range that in both sites it is not possible to determine the coordination number and to distinguish between first and second nearest neighbors. Such large polyhedra are rather uncommon for the lithium cations which usually occupy either tetrahedral or octahedral sites. The Li(1)–O distances vary between 2.234 and 3.319 Å, whereas those corresponding to Li(2) vary between 1.978 and 3.313 Å. The bond strengths of the individual Li–O bonds, calculated by the Brown and Wu method (*17*), are reported in Table VI. They indicate that for Li(1) there are six Li–O distances whose bond strengths are greater than 0.08 and six whose bond strengths are smaller than 0.05. For Li(2), there are three Li–O distances whose bond strengths are greater than 0.22, one for which it is 0.08, and eight whose bond strengths are smaller than 0.05. Consequently, the average Li–O distances (2.746 and 2.736 Å for Li(1) and Li(2), respectively) are much larger than what the ionic radius of the Li^{1+} cation would require. This indicates that the lithium cations do not contribute much to the stability of the structure, but they are mainly needed to balance the electrostatic charge. The existence of compounds such as Ta_3O_7F and

TABLE V

INTERATOMIC DISTANCES (Å)[a]

	Ta(1)—pentagonal bipyramid			
Ta(1)–O(1)	2.107(2)	O(1)–O(2)	2.486	×2
–O(2)	2.067(1) ×2	O(1)–O(4)	2.880	
–O(3)	2.121(2) ×2	O(1)–O(41)	2.835	
–O(4)	1.921(2)	O(2)–O(3)	2.420	×2
–O(41)	1.939(2)	O(2)–O(4)	2.790	×2
Average	2.049	O(2)–O(41)	2.866	×2
Index of distortion	0.085	O(3)–O(3)	2.511	
		O(3)–O(4)	2.819	×2
		O(3)–O(41)	2.915	×2
		Average	2.721	
		Index of distortion	0.193	
	Ta(2)—octahedron			
Ta(2)–O(1)	2.042(1)	O(1)–O(2)	2.486	
–O(2)	2.030(2)	O(1)–O(5)	2.783	
–O(5)	1.919(2)	O(1)–O(7)	2.831	
–O(6)	1.957(2)	O(1)–O(71)	3.000	
–O(7)	1.939(1)	O(2)–O(6)	3.128	
–O(71)	1.981(1)	O(2)–O(7)	2.777	
Average	1.978	O(2)–O(71)	2.702	
Index of distortion	0.049	O(6)–O(5)	2.802	
		O(6)–O(7)	2.642	
		O(6)–O(71)	2.718	
		O(5)–O(7)	2.925	
		O(5)–O(71)	2.763	
		Average	2.796	
		Index of distortion	0.167	
	Ta(3)—octahedron			
Ta(3)–O(2)	2.083(2)	O(2)–O(3)	2.420	
–O(3)	2.014(2)	O(2)–O(6)	2.582	
–O(6)	1.934(2)	O(2)–O(9)	2.935	
–O(8)	1.963(1)	O(2)–O(91)	2.939	
–O(9)	1.953(1)	O(3)–O(8)	3.124	
–O(91)	1.953(1)	O(3)–O(9)	2.891	
Average	1.983	O(3)–O(91)	2.738	
Index of distortion	0.056	O(6)–O(8)	3.075	
		O(6)–O(9)	2.773	
		O(6)–O(91)	2.782	
		O(8)–O(9)	2.695	
		O(8)–O(91)	2.679	
		Average	2.803	
		Index of distortion	0.202	
	Ta(4)—octahedron			
Ta(4)–O(3)	2.020(2) ×2	O(3)–O(3)	2.511	
–O(5)	1.922(2) ×2	O(3)–O(5)	2.828	×2
–O(10)	1.937(3)	O(3)–O(10)	2.873	×2
–O(101)	1.973(3)	O(3)–O(101)	2.759	×2
Average	1.966	O(5)–O(5)	2.928	
Index of distortion	0.046	O(5)–O(10)	2.804	×2
		O(5)–O(101)	2.667	×2
		Average	2.775	
		Index of distortion	0.114	

	Li(1)—polyhedron			
Li(1)–O(3)	3.237(11) ×2	O(3)–O(5)	2.828	×2
–O(5)	2.253(11) ×2	O(3)–O(8)	3.124	×2
–O(6)	3.319(11) ×2	O(3)–O(91)	2.738	×2
–O(8)	2.516(9) ×2	O(3)–O(101)	2.759	×2
–O(71)	2.910(15)	O(5)–O(6)	2.802	×2
–O(9)	2.293(12)	O(5)–O(71)	2.763	×2
–O(91)	2.234(15)	O(5)–O(101)	2.667	×2
–O(101)	2.859(12)	O(6)–O(71)	2.718	×2
Average	2.746	O(6)–O(8)	3.075	×2
Index of distortion	0.451	O(6)–O(9)	2.773	×2
		O(8)–O(9)	2.695	×2
		O(8)–O(91)	2.679	×2
		Average	2.802	
		Index of distortion	0.147	
	Li(2)—polyhedron			
Li(2)–O(2)	2.942(11) ×2	O(2)–O(6)	2.582	×4
–O(2)	3.313(11) ×2	O(2)–O(6)	3.128	×4
–O(6)	2.002(9) ×2	O(2)–O(7)	2.777	×2
–O(6)	2.852(11) ×2	O(2)–O(71)	2.702	×2
–O(7)	2.541(12)	O(2)–O(9)	2.935	×2
–O(71)	1.978(13)	O(2)–O(91)	2.939	×2
–O(9)	3.158(15)	O(6)–O(7)	2.642	×2
–O(91)	2.939(15)	O(6)–O(71)	2.718	×2
Average	2.736	O(6)–O(9)	2.773	×2
Index of distortion	0.494	O(6)–O(91)	2.782	×2
		Average	2.807	
		Index of distortion	0.184	
	Cation–cation separations			
Ta(1)–Ta(1)	3.867	Ta(1)–Li(1)	4.947	×2
–Ta(1)	3.830	–Li(2)	4.700	×2
–Ta(2)	3.284 ×2	Ta(2)–Li(1)	3.403	
–Ta(3)	3.356 ×2	–Li(2)	3.130	
–Ta(4)	3.271	–Li(2)	3.082	
Ta(2)–Ta(2)	3.923	Ta(3)–Li(1)	3.180	
–Ta(2)	3.831	–Li(1)	3.201	
–Ta(2)	3.866	–Li(2)	3.834	
–Ta(3)	3.929	–Li(2)	3.235	
–Ta(3)	3.702	Ta(4)–Li(2)	3.407	×2
–Ta(4)	3.609			
Ta(3)–Ta(3)	3.842	Li(1)–Li(2)	4.192	
–Ta(3)	3.854	Li(2)–Li(2)	3.914	×2
–Ta(3)	3.925			
–Ta(4)	3.839	Li(1)–Li(11)[b]	3.10	
Ta(4)–Ta(4)	3.887	Li(1)–Li(11)[b]	3.87	×2
–Ta(4)	3.810	Li(1)–Li(3)[b]	3.29	
		Li(2)–Li(11)[b]	4.00	
		Li(11)[b]–Li(31)[b]	3.52	
		Li(3)[b]–Li(31)[b]	3.86	×2

[a] In this table the estimated standard deviations for all O–O, Ta–Ta Li–Ta, and Li–Li distances are, respectively, ±0.002, ±0.002, ±0.010, ±0.010.

[b] Distances calculated from estimated center of empty polyhedra.

Nb_2WO_8 seems to give further support to this conjecture. The lithium cations, in order to increase their interaction with the surrounding oxygen anions, have anomalously large temperature factors. This might not necessarily be the result of true thermal

TABLE VI

BOND STRENGTHS AND VALENCES

	O(1)	O(2)	O(3)	O(4)	O(41)	O(5)	O(6)	O(7)	O(71)	O(8)	O(9)	O(91)	O(10)	O(101)	Total valence
Ta(1)	0.61 (0.55) 2×	2 × 0.67 (0.63)	2 × 0.59 (0.53)	2× 0.96 (0.99)	2× 0.92 (0.94)										5.01 (4.80)
Ta(2)	0.71 (0.68)	0.73 (0.70)				0.97 (1.00)	0.88 (0.88)	2× 0.92 (0.94)	2× 0.83 (0.82)						5.04 (5.02)
Ta(3)		0.64 (0.59)	0.76 (0.74)				0.93 (0.95)			2× 0.87 (0.87)	2× 0.89 (0.90)	2× 0.89 (0.90)			4.98 (4.95)
Ta(4)			2 × 0.75 (0.72)			2 × 0.96 (0.99)							2× 0.92 (0.94)	2× 0.85 (0.84)	5.19 (5.20)
Partial valence	2.03 (1.91)	2.04 (1.92)	2.10 (1.99)	1.92 (1.98)	1.84 (1.88)	1.93 (1.99)	1.81 (1.83)	1.84 (1.88)	1.66 (1.64)	1.74 (1.74)	1.74 (1.80)	1.74 (1.80)	1.84 (1.88)	1.70 (1.68)	
Li(1)			2 × 0.03			2 × 0.14	2 × 0.03		1 × 0.05	2× 2 × 0.09	1 × 0.13	1 × 0.14		2× 1 × 0.05	0.95
Li(2)		2 × (0.03 + 0.05)					2 × (0.22 + 0.05)	1 × 0.08	1 × 0.23		1 × 0.03	1 × 0.05			1.09
Li(11)[a]			2×			2×	2×	1×		2×	1×	1×	1×		
Li(3)[a]	2×					4×			2×					1×	
Li(31)[a]	2×					4×		2×					1×		
Total valence	2.03	2.12	2.13	1.92	1.84	2.07	2.11	1.92	1.94	1.92	1.94	1.97	1.84	1.80	

[a] For these sites the type of oxygen anions forming the coordination polyhedra is indicated.

vibrations but could be due to a statistical departure of the lithium ions from the *Pmmn* space symmetry. This additional distortion would not have a long-range order, and the classical diffraction methods would yield an average symmetry for the lithium ions and large thermal vibrations.

Table VI lists the cation–anion bond strengths together with the cation and anion valences. These values were calculated by using the empirical formula, derived by Brown and Wu (*17*), relating bond strengths to bond lengths: $s = (d(1)/d)^n$, where $d(1)$ and n are two constants for a given M–O bond. Their values for Ta–O bonds are 1.907 Å and 5.0, while those for Li–O bonds are 1.378 Å and 4.065. The values shown in Table VI in parentheses represent the bond strengths and the valences calculated by the empirical formula of Zachariasen (*18*): $d = d(1)(1 - A \ln \cdot s)$, where $d(1)$ and A are two constants for each M–O bond. Since the $d(1)$ and A values for Li–O bonds were not reported by Zachariasen, only the strengths of the Ta–O bonds and the tantalum valences have been calculated by this method. The $d(1)$ and A values used were 1.918 Å and 0.166, respectively. As can be seen from Table VI the bond strength and valence values calculated by the two methods are in good qualitative agreement with each other. The Ta(1), Ta(2), and Ta(3) cations have valences close to 5, whereas a slightly higher value (5.19) is obtained for Ta(4) by both methods. This chemically unfeasible value could be explained by the large thermal motion of Ta(4) along the *b* axis. It has been shown that large thermal motions tend to decrease the apparent bond length as determined by diffraction methods and to increase the bond strength and consequently the valence (*19*). The anion valences, calculated by the Brown and Wu method, range between 1.80 and 2.13. With the exception of O(10) and O(101), the anion valences differ by no more than 7% from the expected value of 2.00. This indicates that there is nearly perfect valence balance throughout the structure. Although O(10) and O(101) are not severely underbonded (the calculated valence is 1.84 and 1.80, respectively), their underbonding might be used to explain the large anisotropy of Ta(4) along the *b* axis. It must be pointed out that O(101) is strongly bonded to two Ta(4) and weakly bonded to two Li(1), while O(10) is strongly bonded to two Ta(4) only. The bonds Ta(4)–O(101) and Ta–O(10) are both along the *b* axis. It is evident that Ta(4) cannot be closer to one of the two oxygen ions than to the other, otherwise the second would become severely underbonded. Thus it remains in the middle, and since both oxygen ions are slightly underbonded, it compensates this small valence imbalance by vibrating along the bond direction.

It can be seen from Table VI that if Li(11) would exist, it would be bonded to the same oxygen atoms to which Li(1) is bonded, except for O(71) and O(101), which are bonded to Li(1) only, and for O(7) and O(10) which would be only bonded to the Li(11). Because of this similarity, if both sites were occupied, then the 10 common oxygen atoms would become severely overbonded. On the other hand, it should be noted that the sites of Li(3) and Li(31) would not be enough to completely fill the valence deficiency of the underbonded oxygen atoms. For instance, if one considers as deficient those oxygen atoms whose valence, calculated from the Ta–O bonds only, is less than 1.90, then Li(1), Li(2), and Li(11) (if it would exist) are bonded to eight of these deficient oxygen atoms, whereas Li(3) and Li(31) are bonded to only three. By occupying either sites 1 and 2 or sites 11 and 2, the lithium atoms cause the smallest distortion due to electrostatic imbalance. It should be pointed out that the superstructure is due to the fact that sites 1 and 11 cannot be occupied simultaneously.

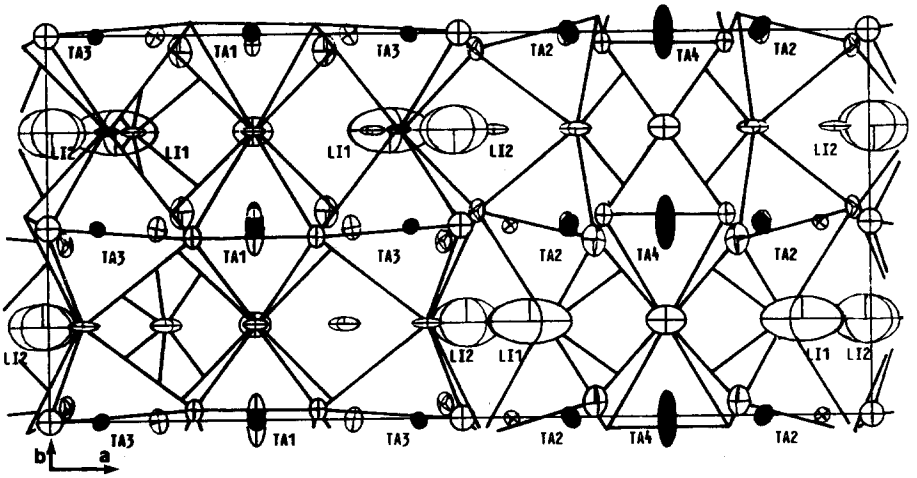

FIG. 6. Projection of the crystal structure of H-$LiTa_3O_8$ along the c axis. Each atom is represented by the section of its thermal ellipsoid perpendicular to the c axis. Oxygen polyhedra around the tantalum cations are outlined.

Along the cuboctahedral chains formed by sites 1 and 11, every other site is empty; namely, sites 1 are full and sites 11 are empty. The cuboctahedral sites of the Li(2) chains are all full, while the 9-coordinated polyhedra of the chains formed by the sites 3 and 31 are all empty. Because of their weak bonding to the oxygen ions of the $Ta_3O_8^{1-}$ framework and the existence of neighboring empty sites, the lithium cations are apt to become mobile with increasing temperature and therefore to be responsible for the ionic conductivity. The three empty sites are equivalent in size to the two full sites. If one calculates the distances from the center of the empty polyhedra to the oxygen atoms forming them, the following values are obtained for the average distances: (site 11)–O = 2.812 Å, (site 3)–O = 2.417 Å, and (site 31)–O = 2.483 Å. These values are to be compared with Li(1)–O = 2.746 Å and Li(2)–O = 2.736 Å. The Li(1) cations can hop to four adjacent sites, namely three 11 and one 3, whereas the Li(2) cations can only hop to one adjacent 11 site. The hopping takes place through distorted rhombic holes formed by oxygen atoms. For instance, the Li(1) cation at (0.41, 0.75, 0.09) can hop to the site 31 at (0.25, 0.75, 0.25) through the rhombus formed by the O(5), O(71), O(5), and O(101). The O(5)–O(5) and O(71)–O(101) diagonals are already long enough at room temperature (3.227 and 4.311 Å, respectively) to allow the lithium hopping from site 1 to site 31. A lithium cation which has moved to a 31 site can continue its hopping on going along the empty chains formed by sites 31 and 3. This hopping would take place through the triangular holes formed by the O(5), O(1), and O(5) anions. At room temperature the three edges of the triangle are 2 × O(1)–O(5) = 2.783 Å and O(5)–O(5) = 2.928 Å, which are rather small. It is conceivable that the size of the triangles and the rhombi would increase with increasing temperature. Once the lithium cations begin to move, hopping from a given site to one previously occupied might take place. All possible hoppings and the room-temperature size of the corresponding holes are given in Table VII, and they can be visualized from Fig. 2. The distribution of the lithium sites throughout the structure and the hoppings which might take place, clearly demonstrate that the high-tempera-

TABLE VII

LITHIUM HOPPINGS

Hopping From	Hopping To and vice versa	Occupancy at room temp.		Oxygen anions forming the holes	Diagonal distances or triangular edges (Å)
Site (1)	Site (11)	Full	Empty	O(5)–(6)–(8)–(3)	O(5)–O(8) = 3.206; O(6)–O(3) = 4.873
(1)	(11)	Full	Empty	O(9)–(8)–(91)–(8)	O(9)–O(91) = 3.697; O(8)–O(8) = 3.849
(1)	(3)	Full	Empty	O(5)–(71)–(5)–(101)	O(5)–O(5) = 3.227; O(71)–O(101) = 4.312
(1)	(2)	Full	Full	O(6)–(9)–(6)–(71)	O(6)–O(6) = 4.453; O(9)–O(71) = 3.131
(2)	(11)	Full	Empty	O(6)–(91)–(6)–(7)	O(6)–O(6) = 3.244; O(91)–O(7) = 4.171
(11)	(31)	Empty	Empty	O(5)–(7)–(5)–(10)	O(5)–O(5) = 4.470; O(7)–O(10) = 3.254
(3)	(31)	Empty	Empty	O(5)–(1)–(5)	2 × O(5)–O(1) = 2.783; O(5)–O(5) = 2.928
(2)	(2)	Full	Full	O(6)–(2)–(6)–(2)	O(6)–O(6) = 2.993; O(2)–O(2) = 4.893

ture form of $LiTa_3O_8$ is a tridimensional ionic conductor as found experimentally by Magniez (*9*). However, it is surprising that quenching from high temperature does not preserve any sign of this hopping, and all Li^+ ions settle into their respective room-temperature sites. Probably high-temperature neutron diffraction is needed to clarify this point.

It has been stated in the introduction that the ionic conductivity of solid solutions such as $Li_{1-x}Ta_3O_{8-x}F_x$ and $Li_{1-x}Ta_{3-x}W_xO_8$ attains a maximum in both cases for $x = 0.75$. A priori one cannot determine whether $LiTa_{12}O_{29}F_3$ and $LiTa_9W_3O_{32}$ belong to the *Pmma* space group or to *Pmmn*. In the former space group, any lithium site would be partially occupied. If only one type of sites is occupied, then sites 2 or 3 would have a 0.50 occupation factor, while sites 1 would have 0.25 occupancy. In the case of the *Pmmn* space group, if the lithium cations occupy only one type of site, then sites 1 or 11 or 2 would have a 0.50 occupation factor, whereas sites 3 or 31 would be fully occupied. Since high ionic conductivity is usually associated with partially occupied sites, it is likely that the Li^{1+} ions would be in positions partially occupied rather than in the fully occupied sites 3 and 31.

The anisotropic vibrations of all atoms are shown in Figs. 5 and 6. A qualitative study of these results reveals several features of physical interest and significance. One sees, for instance, that the lithium cations have thermal amplitudes larger than the oxygen atoms, which in turn show displacements larger than those of the tantalum cations, except for that of Ta(4) along the *b* axis. This large thermal vibration has been explained above as due to the underbonding of O(10) and O(101), whose bonds to Ta(4) are along the *b* axis. The size of the oxygen octahedron around Ta(4) is quite suitable for the radius of the Ta^{5+} cations; therefore, the large thermal vibrations are not due to a size effect.

The lithium cations also have large thermal vibrations, but in their case their vibrations are indeed the result of a size effect. The oxygen anions, which belong to the plane containing the lithium cations, namely the plane at $y = \frac{1}{4}$, have larger thermal vibrations than the oxygen ions belonging to the plane at $y \simeq 0$ containing the tantalum cations. Furthermore, the thermal vibrations of the oxygen ions of the $y = \frac{1}{4}$ plane are strongly anisotropic, and the directions of the maximum thermal displacement are nearly parallel to the directions of the corresponding Li–O bonds.

The values of the anisotropic thermal factors and the orientation of tensor ellipsoids are consistent with the directions and strengths of the chemical bonds.

Acknowledgments

The authors thank Professor M. Alario-Franco for the use of the electron microscope at the CSIC in Marid and for helpful discussions. They also thank the Laue-Langevin Institute at Grenoble for its hospitality while performing the experiment with the neutron Weissenberg camera.

References

1. R. S. ROTH, H. S. PARKER, W. S. BROWER, AND J. L. WARING, "Fast Ion Transport in Solids," Proceedings of the NATO Sponsored Advanced Study Institute, Belgirate, Italy, September 1972, North-Holland, Amsterdam (1973).
2. B. M. GATEHOUSE, private communication to R. S. Roth, as quoted in Ref. (*1*).
3. M. LUNDBERG, *Acta Chem. Scand.* **19,** 2274 (1965).
4. B. G. HYDE, A. N. BAGSHAW, S. ANDERSSON, AND M. O'KEEFE, *Amer. Rev. Mater. Sci.* **4,** 43 (1974).
5. A. G. NORD AND J. O. THOMAS, *Acta Chem. Scand. Ser. A* **32,** 539 (1978).
6. G. D. FALLON, B. M. GATEHOUSE, R. S. ROTH, AND S. A. ROTH, *J. Solid State Chem.* **27,** 255 (1979).
7. P. E. WERNER, B. O. MARINDER, AND A. MAGNELI, *Mater. Res. Bull.* **13,** 1371 (1978).
8. J. M. RÉAU, G. MAGNIEZ, L. RABARDEL, J. P. CHAMINADE, M. POUCHARD, AND A. HAMMOU, *Mater. Res. Bull.* **11,** 867 (1976).
9. G. MAGNIEZ, Thèse d'Etat, Université de Bordeaux I (1976).
10. J. M. RÉAU, G. MAGNIEZ, J. P. CHAMINADE, M. POUCHARD, AND P. HAGENMULLER, *Acta Chem. Scand. Ser. A* **31,** 98 (1977).
11. J. L. HODEAU, M. MAREZIO, A. SANTORO, AND R. S. ROTH, Collected Abstracts, 1-D-16, Sixth European Crystallographic Meeting, Barcelona, Spain (1980).
12. E. PRINCE, National Bureau of Standards U.S. Technical Note 1117, edited by F. Shorten (1980).
13. G. CAGLIOTI, A. PAOLETTI, AND F. P. RICCI, *Nucl. Instrum.* **3,** 223 (1958).
14. G. E. BACON, *Acta Crystallogr. Sect. A* **28,** 357 (1972).
15. A. W. HEWAT, ILL Report 74H625, Grenoble, France (1974).
16. P. J. BECKER AND P. COPPENS, *Acta Crystallogr. Sect. A* **30,** 129 (1974).
17. I. D. BROWN AND K. K. WU, *Acta Crystallogr. Sect. B* **32,** 1957 (1976).
18. W. H. ZACHARIASEN, *J. Less-Common Met.* **62,** 1 (1978).
19. I. D. BROWN AND R. D. SHANNON, *Acta Crystallogr. Sect. A* **29,** 266 (1973).